Available online at www.sciencedirect.com
ScienceDirect
International Journal of Pharmaceutics 342 (2007) 194–200
INTERNATIONAL JOURNAL OF PHARMACEUTICS
www.elsevier.com/locate/ijpharm

Pharmaceutical Nanotechnology

Tumor targeting of doxorubicin by anti-MT1-MMP antibody-modified PEG liposomes

Hiroto Hatakeyama [a], Hidetaka Akita [a], Emi Ishida [b], Koichi Hashimoto [b], Hideo Kobayashi [b], Takanori Aoki [c], Junko Yasuda [c], Kenichi Obata [c], Hiroshi Kikuchi [b], Tatsuhiro Ishida [d], Hiroshi Kiwada [d], Hideyoshi Harashima [a,*]

[a] *Graduate School of Pharmaceutical Sciences, Hokkaido University, Sapporo, Hokkaido 060-0812, Japan*
[b] *Daiichi Pharmaceutical Co. Ltd., Tokyo 134-8630, Japan*
[c] *Daiichi Fine Chemical Co. Ltd., Takaoka, Toyama 933-8511, Japan*
[d] *Faculty of Pharmaceutical Sciences, The University of Tokushima, Tokushima 770-8505, Japan*

Received 27 October 2006; received in revised form 23 March 2007; accepted 24 April 2007
Available online 10 May 2007

Abstract

Immunoliposomes are potent carriers for targeting of therapeutic drugs to specific cells. Membrane type-1 matrix metalloproteinase (MT1-MMP), which plays an important role in angiogenesis, is expressed on angiogenic endothelium cells as well as tumor cells. Then, the MT1-MMP might be useful as a target molecule for tumor and neovascularity. In the present study, we addressed a utility of antibodies against the MT1-MMP as a targeting ligand of liposomal anticancer drug. Fab′ fragments of antibody against the MT1-MMP were modified at distal end of polyethylene glycol (PEG) of doxorubicin (DXR)-encapsulating liposomes, DXR-sterically stabilized immunoliposomes (DXR-SIL[anti-MT1-MMP(Fab′)]). Modification with the antibody significantly enhanced cellular uptake of DXR-SIL[anti-MT1-MMP(Fab′)] into the HT1080 cells, which highly express MT1-MMP, compared with the non-targeted liposomes (DXR-stealthliposomes (DXR-SL)), suggesting that MT1-MMP antibody (Fab′) is a potent targeting ligand for the MT1-MMP expressed cells. *In vivo* systemic administration of DXR-SIL[anti-MT1-MMP(Fab′)] into the tumor-bearing mice showed significant suppression of tumor growth compared to DXR-SL. This is presumably due to the active targeting of immunoliposomes for tumor and neovascularity. However, tumor accumulation of DXR-SIL[anti-MT1-MMP(Fab′)] and DXR-SL were comparable, suggesting that both liposomal formulations accumulated in tumor via enhanced permeation and retention (EPR) effect, but not via targeting to the MT1-MMP expressed on both the endothelial and tumor cells. It appears that the enhanced antitumor activity of DXR-SIL[anti-MT1-MMP(Fab′)] resulted from acceleration of cellular uptake of lioposomes owing to the incorporated antibody after extravasation from capillaries in tumor.

Keywords: Immunoliposomes; Cancer therapy; Drug delivery; Matrix metalloproteinase

1. Introduction

Sterically stabilized polyethyleneglycol (PEG)-modified liposomes have already been optimized for escaping uptake by reticuloendothelial system (RES) and prolonging systemic circulation (Klibanov et al., 1990), which resulted in increased accumulation in tumor tissue by enhanced permeation and retention (EPR) effect (Matsumura and Maeda, 1986). Notably, PEGylated liposomes encapsulating doxorubicin (Doxil®) are currently used in clinics. Targeting of liposomes to specific cells is a promising strategy for reducing side effects and improving therapeutic effects. To date, immunoliposomes, in which antibodies were conjugated at the distal end of PEG, were used as carriers. For example, antibodies against vascular cell adhesion molecule-1 (VCAM-1) (Voinea et al., 2005) and insulin receptor (Zhang et al., 2003) for inflammatory tissue and brain, respectively, and epidermal growth factor receptor (EGFR) (Mendelsohnand and Baselga, 2003), transferrin receptors (TfR) (Pardridge, 2004; Xu et al., 2002) were utilized as targets for the cancer cells. Furthermore, the modification of Doxil® with antinuclear autoantibodies against nucleosomes possesses an ability

* Corresponding author at: Faculty of Pharmaceutical Sciences, Hokkaido University, Sapporo, Hokkaido 060-0812, Japan. Tel.: +81 11 706 3919; fax: +81 11 706 4879.
E-mail address: harasima@pharm.hokudai.ac.jp (H. Harashima).

0378-5173/$ – see front matter © 2007 Elsevier B.V. All rights reserved.
doi:10.1016/j.ijpharm.2007.04.037

to specifically recognize the surface of numerous tumor cells, but not normal cells (Lukyanov et al., 2004). Generally, immunoliposomes modified with Fab′ fragment exhibit longer systemic circulation compared with that modified with whole IgG since RES uptakes immunoliposomes via the Fc receptor-mediated mechanism (Maruyama et al., 1997).

Recent progress in cancer physiology revealed that tumor growth is closely related to the development of new blood vessels. Then, inhibition of neovascularity is a potent strategy for cancer therapy. One of the key proteins on angiogenesis in tumor vessels is membrane type-1 matrix metalloproteinase (MT1-MMP), which is expressed on the neovascularity as well as tumor cells. On the plasma membrane, MT1-MMP cleaved extracellular matrix components such as collagen, laminin, fibronectin and elastin (Knauper et al., 1996; Noel et al., 1995; Ohuchi et al., 1997; Pei et al., 1994; Pei and Weiss, 1996; Sato et al., 1994; Strongin et al., 1995). Simultaneously, MT1-MMP activates soluble MMPs (i.e. MMP-2) via its proteolytic activity, which also plays an important role in the degradation of the matrix (Knauper et al., 1996; Ohuchi et al., 1997; Pei and Weiss, 1996; Sato et al., 1994; Strongin et al., 1995). In fact, administration of the inhibitors for MMP families to the tumor-bearing mouse suppressed the angiogenesis, which resulted in the antitumor effect (Maekawa et al., 1999; Nelson, 1998). Based on previous report, dual targeting of antitumor drugs to the neovascular cells and tumor cells are expected to be excellent strategy for the cancer therapy (Maeda et al., 2004). To realize this strategy, we established the doxorubicin-encapsulating sterically stabilized immunoliposome (DXR-SIL[anti-MT1-MMP(Fab′)]), in which Fab′ fragment ($Fab'_{222\text{-}1D8}$) derived from anti-human MT1-MMP monoclonal antibody was modified at the distal end of PEG. In the present study, utility of these immounoliposomes were assessed in both *in vitro* cellular uptake and *in vivo* antitumor effect between DXR-SIL[anti-MT1-MMP(Fab′)] and non-targeted doxorubicin-encapsulating sterically stabilized liposomes (DXR-SL).

2. Methods and materials

2.1. Materials

Cholesterol (CH), distearoyl-*sn*-glycero-3-phoshoethanolamine-*N*-[methoxy(polyethylene glycol)-2000] (DSPE-PEG), hydrogenated soy phosphatidylcholine (HSPC), cysteamine hydrochloride were purchased from WAKO (Osaka, Japan), Genzyme (Cambridge, MS, USA) and Lipoid (Ludwigshafen, Germany). DSPE-PEG with a functional maleimide moiety at the terminal end of PEG: *N*-[(3-maleimide-1-oxopropyl)aminopropyl polyethyleneglycol-carbamyl] distearoyllphosphatidyl-ethanolamine (DSPE-PEG-Mal) was purchased from Shearwater (Enschede, The Netherlands). Doxorubicin (DXR) was purchased from Sicor Inc. (Irvine, CA, USA). Ultrogel Ac54 and Sepharose CL-5B were purchased from Pall Biosepra (St. Christophe, France) and Amersham Pharmacia (Arlington Heights, IL, USA). *N*-Ethylmaleimide was purchased from Nacalai Tesque (Kyoto, Japan).

2.2. Animal and cell line

Male BALB/c nude mice (5–6 weeks old) were purchased from CLEA Japan (Tokyo, Japan). All *in vivo* experiments were approved by the Institutional Animal Care and Use Committee. HT1080 cells were purchased from RIKEN Cell Bank and cultured in DMEM supplemented with 10% fetal bovine serum (FBS), penicillin (100 U/ml), streptomycin (100 μg/ml) at 37 °C with 5% CO_2 and 95% humidity on the bottom of a dish (Corning).

2.3. Preparation of Fab′ fragment

Fab′ fragment was prepared from anti-MT1-MMP monoclonal antibody (222-1D8) (Aoki et al., 2002). A volume of 1 ml of the IgG (10 mg/ml) was dialyzed against 0.1 M sodium acetate buffer (pH4.2) containing 0.1 M NaCl, and then added with pepsin at a concentration of 2% (w/w) based on the amount of antibodies and digested at 37 °C. After the incubation for 20 h, the digested product was added with 0.2 ml of 3 M Tris–HCl (pH7.5) to terminate the reaction. The whole digestion product was loaded on an Ultrogel AcA54 gel filtration column (diameter 1.5 cm × length 47 cm) equilibrated with 0.1 M phosphate buffer (pH 7.0) and collected as 1 ml fractions. Elution of $F(ab')_2$ was monitored by UV adsorption (A280). The resulting $F(ab')_2$ was adjusted to a volume of 0.9 ml with 0.1 M phosphate buffer (pH 6.0), supplied with 0.1 ml of 0.1 M cysteamine hydrochloride (final concentration: 0.01 M) and thereby reduced at 37 °C for 1.5 h. The resultant was loaded on an Ultrogel AcA54 gel filtration column (diameter 1.5 cm × length 47 cm) equilibrated with PBS containing 5 mM EDTA and collected as 1 ml fractions. The elution of Fab′ was monitored by A280.

2.4. Preparation of immunoliposomes (DXR-SIL[anti-MT1-MMP(Fab′)])

Lipid film composed of 47.4 mM HSPC/CH (6:4 molar ratio) was prepared by the evaporation. The lipid film was hydrated with 155 mM ammonium sulfate at pH 5.5, and then particle size of liposomes was controlled by sequential extrusion through polycarbonate membrane filter of 0.2, 0.1, 0.05 μm pore diameter. The extruded liposomes were centrifuged at 300,000 × *g* for 1 h at 4 °C and then resuspended in saline. DXR or [^{14}C]-labeled DXR ([^{14}C]-DXR) was incubated with actively loaded into the liposomes following an ammonium sulfate gradient as described previously (Haran et al., 1993). Then, liposomes were PEGylated by incubating with 0.25 mM of DSPE-PEG or DSPE-PEG/DSPE-PEG-Mal (9:1 molar ratio) for 15 min at 65 °C. Sterically stabilized liposomes (DXR-SL) were centrifuged at 300,000 × *g* for 1 h at 4 °C to remove unloaded DXR and then resuspended in saline to remove unloaded DXR.

To conjugate the Fab′ fragment (1.96 mg/0.37 ml), 0.41 ml of maleimide-introduced liposomes (maleimide concentration: 104 nmol/ml) were mixed with Fab′ fragment (the molar ratio of maleimide moiety and Fab′ fraction was 3:1). After the incubation for 20 h at 4 °C under light shielding, unreacted mercapto groups were blocked by adding 4.3 μl of 0.1 M *N*-

ethylmaleimide. To remove free Fab′ fragment, the reaction mixture was loaded on an Sepharose CL-4B gel filtration column (diameter 3 cm × length 50 cm) equilibrated with PBS and collected as 2 ml fractions. The concentration of cholesterol was quantified by cholesterol *E*-test WAKO kit (Wako: Osaka, Japan). The particle size of liposomes was determined by dynamic light scattering (DLS) (ELS-8000, Otsuka Electronics, Japan).

2.5. In vitro cellular uptake study

To visually compare the cellular uptake of DXR-SIL[anti-MT1-MMP(Fab′)] and DXR-SIL, 5×10^4 cells/dish of HT1080 cells were plated into 3.5 cm dish. DXR-SL or DXR-SIL[anti-MT1-MMP(Fab′)] (14.5 μM of total lipid) were applied and incubated for 3 h at 37 °C, and then washed by Krebs-Henseleit buffer (118 mM NaCl, 23.8 mM $NaHCO_3$, 4.83 mM KCl, 0.96 mM KH_2PO_4, 1.20 mM $MgSO_4$, 12.5 mM HEPES, 5 mM glucose, and 1.53 mM $CaCl_2$ adjusted to pH 7.4). Images were collected by confocal laser scanning microscopy (CLSM) (LSM510 META, Carl Zeiss, Germany). For the quantitative cellular uptake analysis, cells were seeded in 12-well plates at a density of 4×10^4 cells/well 24 h before the transport assay. All transport assays were performed in Krebs-Henseleit buffer. The cells were washed by Krebs-Henseleit buffer. The [^{14}C]-DXR-SIL[anti-MT1-MMP(Fab′)] and [^{14}C]-DXR-SL were added to the Krebs-Henseleit buffer (14.5 μM of total lipid), followed by incubation for 10 min, 1 h and 3 h at 37 °C. Just before the designated times, 50 μl Krebs-Henseleit buffer was transferred to scintillation vials. Then cells were washed with 2 ml ice-cold Krebs-Henseleit buffer to remove the liposomes binding to cell surface and solubilized in 500 μl 1N NaOH. After adding 250 μl 2N HCl, 500 μl aliquots were transferred to scintillation vials. The radioactivity of the cells and Krebs-Henseleit buffer was determined by liquid scintillation counting (LS 6000SE; Beckman Instruments Inc., Fullerton, CA, USA) after 4.5 ml scintillation fluid (Hionic fluor; Packard Instrument Co., Downers Grove, IL, USA) was added to the scintillation vials. The remaining 100 μl aliquots of cell lysate were used to determine protein concentrations by the BCA protein assay kit (PIERCE, Rockford, IL, USA) with BSA as a standard. The uptake of liposomes is given as the volume of distribution, determined as the amount of ligands associated with the cells normalized by the medium concentration.

2.6. Evaluation of in vivo pharmacological effect

Tumor-bearing mice were prepared by s.c. inoculation of a suspension (1×10^6 cells per 100 μl PBS) of HT1080 into BALB/c nude mice. DXR-SIL[anti-MT1-MMP(Fab′)] and DXR-SL were administered at a dose of 3 mg/kg DXR (corresponding to 5 μmol lipid/mouse) to tumor-bearing mice via the tail vein when tumor size was in the range from 1000 to 3000 mm^3. The tumor size was measured up to 12 days after administration. Data were represented as a relative tumor volume normalized by that when liposomes were injected. The antitumor effect was defined as the percent of tumor volume at the indicated times to that at day 0.

2.7. Comparison of in vivo tumor distribution

[^{14}C]-DXR-SIL[anti-MT1-MMP(Fab′)] and [^{14}C]-DXR-SL at a dose of 0.15 μmol lipid/mouse was injected to tumor-bearing mice from the tail vein at 11 days after tumor implantation. At 48 h post-injection, the mice were sacrificed and blood and tumor tissue were collected. The blood and tumor sample were solubilized in Soluene-350 for 5 h at 50 °C. The solubilized blood sample was decolorized by H_2O_2. The radioactivities were determined by liquid scintillation counter with Hionic Fluor.

3. Results and discussion

3.1. Characterization of immunoliposomes

The average particle size of DXR-SIL[anti-MT1-MMP(Fab′)] and DXR-SL was in the range of 85–90 nm and encapsulated ratio of DXR was >97%. The number of Fab′ fragment attached to the distal end of the PEG was approximately 40 molecules, which was calculated as described previously (Hatakeyama et al., 2004).

3.2. Comparison of in vitro cellular uptake

The cellular uptake of DXR encapsulated in SIL[anti-MT1-MMP(Fab′)] and SL by the MT1-MMP-expressing HT1080 cells was compared (Fig. 1). In CLSM analysis, fluorescence signal of DXR was only a slightly detected in SL, whereas strong fluorescence of DXR was detected in SIL[anti-MT1-MMP(Fab′)] (Fig. 1A). The modification with the antibody accelerated cellular uptake of the liposomes. In the quantitative cellular uptake study, the cellular uptake of the both liposomes was increased in time-dependent manner and was stimulated by the modification with Fab′ by approximately five-fold, as compared with non-targeted liposomes (DXR-SL) (Fig. 1B). Since DXR is hydrophobic, it can efficiently diffuse into the cells. However, it is confirmed that leakage of encapsulated DXR in the medium was negligible (retention efficiency >97%, up to 24 h). Collectively, these data indicated that DXR-SIL[anti-MT1-MMP(Fab′)] is efficiently bound to the MT1-MMP-expressing cells, and then is internalized. Considering that the function of MT1-MMP was regulated by endocytosis and recycling (Itoh and Seiki, 2004; Uekita et al., 2001; Wang et al., 2004), the DXR-SIL[anti-MT1-MMP(Fab′)] was also taken up via receptor-mediated endocytosis.

3.3. Comparison of antitumor effect

DXR-SL shows more efficient anti-cancer effects than free DXR, since free DXR are distributed in various organs in non-specific manner (Čeh et al., 1997). To address the utility of DXR-SIL[anti-MT1-MMP(Fab′)] from the view point of *in vivo* antitumor effect, DXR-SIL[anti-MT1-MMP(Fab′)] and DXR-SL were intravenously administered to the tumor-bearing mice

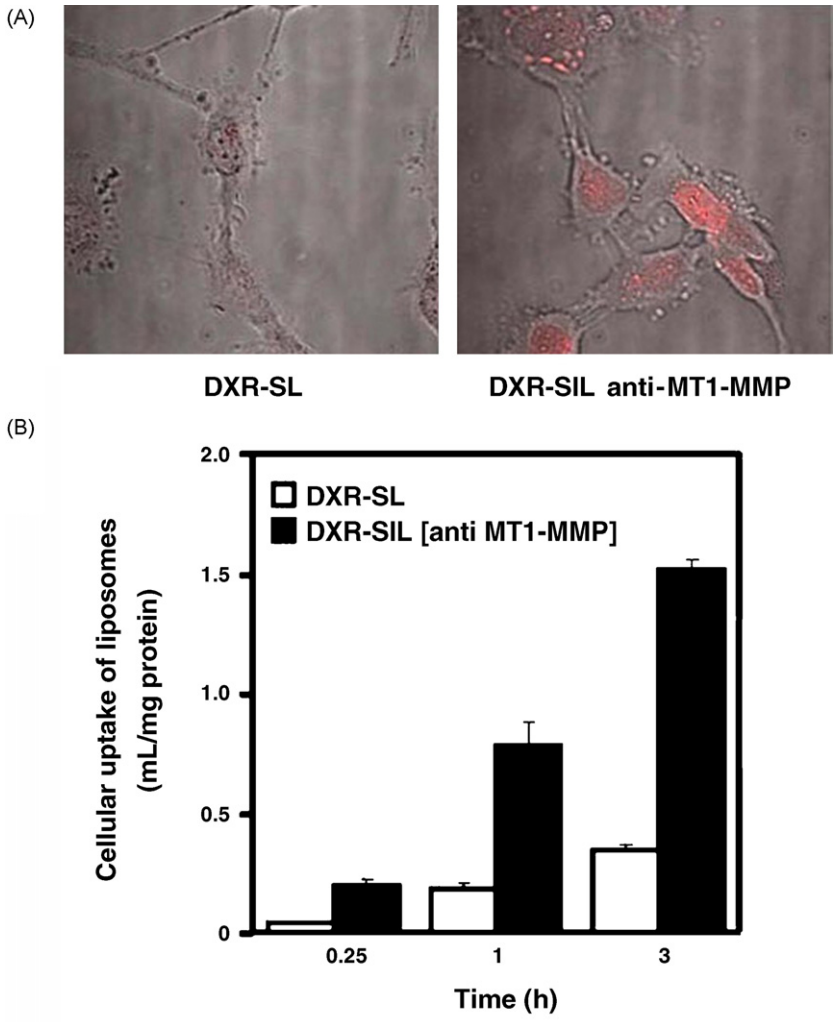

Fig. 1. Cellular uptake of DXR-SIL[anti-MT1-MMP(Fab′)] and DXR-SL to the HT1080 cells. (A) DXR-SIL[anti-MT1-MMP(Fab′)] (right panel) and DXR-SL (left panel) were incubated with HT1080 cells for 3 h. Cells were washed, and then intracellular accumulation of encapsulated doxorubicin was fluorescently visualized with CLSM. (B) [^{14}C]-DXR-SIL[anti-MT1-MMP(Fab′)] (closed bars) and DXR-SL (opened bars) were incubated with HT1080 cells. At indicated time, cells were washed and then cellular radioactivity was counted by liquid scintillation counter. Cellular radioactivity was normalized by the protein amount of the sample. Data were represented as mean ± S.D. ($n = 3$).

($n = 6$), respectively. Fig. 2 showed the time profiles for the relative tumor volume up to 12 days after administration of liposomal formulations. When DXR-SL was administered, tumor volume was decreased in only 1 out of 6 mice at 12 days (Fig. 2A). Furthermore, three of six mice died up to 12 day, the body weights of which were drastically decreased (14.8%, 17.7%, and 17.8%, respectively), presumably by the side effect of DXR-SL. In contrast, in the case of DXR-SIL[anti-MT1-

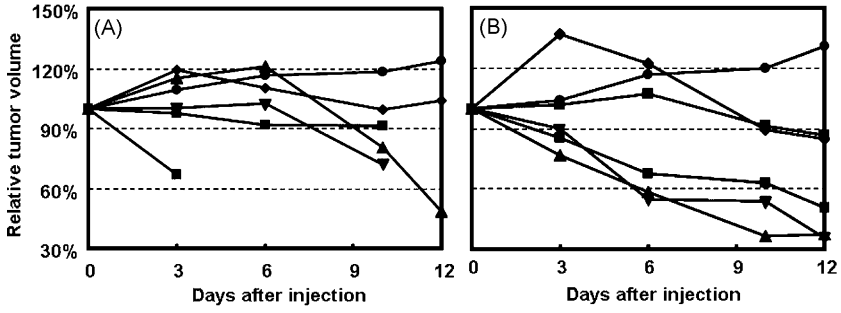

Fig. 2. Time profiles of the tumor volume after the single i.v. injection of DXR-SIL[anti-MT1-MMP(Fab′)] and DXR-SL. DXR-SIL[anti-MT1-MMP(Fab′)] and DXR-SL were injected from tail vein at a dose of 3 mg/kg DXR and 5 μmol lipid/mouse. Tumor volume was measured just before the injection, and up to 12 days after the injection. The data of six individual mice were plotted. (A) and (B) represented the data after the injection of DXR-SL and DXR-SIL[anti-MT1-MMP(Fab′)], respectively.

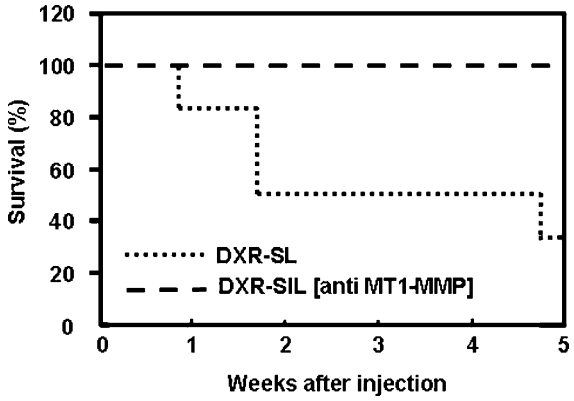

Fig. 3. Time profiles for the survival rate of mice after the single injection of DXR-SIL[anti-MT1-MMP(Fab′)] and DXR-SL. After the single i.v. administration of DXR-SIL[anti-MT1-MMP(Fab′)] and DXR-SL, survival of six mice was followed up until 5 weeks.

MMP(Fab′)], tumor volume decreased efficiently in half of mice at 12 days (Fig. 2B). Furthermore, whereas one mouse showed notably body weight change (20.1%), no mouse died. These results suggested that DXR-SIL[anti-MT1-MMP(Fab′)] would be superior to that of DXR-SL from the point of view of antitumor activity and less side effect. As shown in Fig. 3, administration of DXR-SIL [anti-MT1-MMP] exhibited prolonged survival compared with that of DXR-SL, presumably because of the temporal inhibition of tumor growth after the administration. These data suggested that DXR-SIL [anti-MT1-MMP] was more potent in the pharmacological activity than that of DXR-SL.

3.4. Comparison of in vivo tumor distribution

The amino acid sequence of human MT1-MMP is highly homologous approximately 96% matching with mouse MT1-MMP. Therefore, it is plausible that 222-1D8 cross-react with mouse MT1-MMP. Considering that MT1-MMP was expressed on the neovascular membrane, more potent antitumor activity can be attributed to the efficient accumulation of the liposomes via the targeting function of the Fab′ fragment. To measure the distribution of DXR in the tumor, [^{14}C]-DXR-SIL[anti-MT1-MMP(Fab′)] and [^{14}C]-DXR-SL were administered intravenously, and then radioactivities in blood sample and tumor were measured after 48 h. As a result, blood concentration of DXR encapsulated in SIL[anti-MT1-MMP(Fab′)] and in SL was comparable, indicating that modification of $Fab'_{222\text{-}1DB}$ did not alter the tumor accumulation of these liposomes (Fig. 4A). This is inconsistent with a previous observation in OX-26-modified PEG liposomes (Huwyler et al., 1996), which is designed as the targeting vector for transferrin receptor (TfR)-expressing organs. In that study, OX-26-modified immunosterically stabilized liposomes were rapidly eliminated from the blood circulation compared with non-targeted sterically stabilized liposomes, when more than 20 of OX-26 antibodies were conjugated. In contrast, in the present study, retention of DXR-SIL[anti-MT1-MMP(Fab′)] in the blood circulation was comparable even though the DXR-SIL[anti-MT1-MMP(Fab′)] were expected to have approximately 40 of $Fab'_{222\text{-}1DB}$. The antibody-dependent difference in the blood concentration of liposomes may be accounted for by the tissue distribution of transferrin receptor and MT1-MMP. Since transferrin receptors were ubiquitously and widely expressed at various organs (Hatakeyama et al., 2004; Ponkaand and Lok, 1999; Qian et al., 2002), systemic OX-26-modified immunoliposomes may be cleared by various organs, in addition to the RES. In contrast, the expression of MMPs remained few at normal condition and induced only at the pathological condition such as inflammation and malignant alternation (Sato et al., 1994; Pagenstecher et al., 1998). It is likely that clearance of the $Fab'_{222\text{-}1DB}$-modified immune-sterically stabilized liposomes (SIL[anti-MT1-MMP(Fab′)]) was mainly governed by RES as is the case of non-targeted liposomes (SL).

Then, tumor accumulation of DXR-SIL[anti-MT1-MMP(Fab′)] was compared with DXR-SL at 48 h after intravenous administration. Unexpectedly, the accumulation of DXR-SIL[anti-MT1-MMP(Fab′)] was comparable or slightly lower than that of DXR-SL, although MT1-MMP should be expressed in the neovascular membrane. This result is

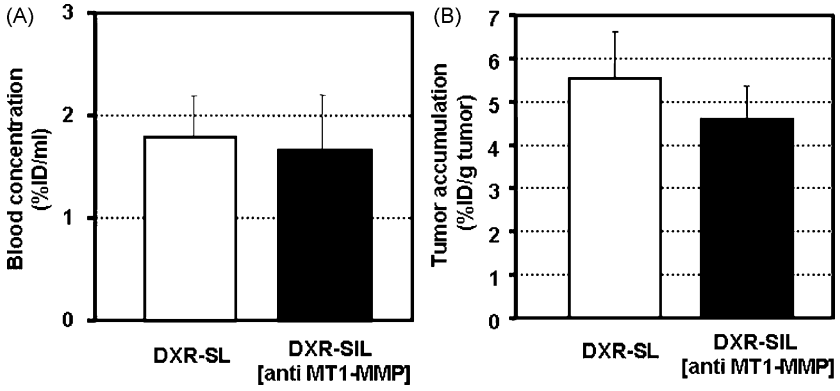

Fig. 4. Blood concentration and tumor accumulation of [^{14}C]-DXR-SIL[anti-MT1-MMP(Fab′)] and [^{14}C]-DXR-SL. At 48 h post-injection of [^{14}C]-DXR-SIL[anti-MT1-MMP(Fab′)] and DXR-SL at a dose of 0.15 μmol lipids/mouse, the mice was sacrificed and blood and tumor were collected. Radioactivities in the blood and tumor tissue were determined by liquid scintillation counter. The data of blood concentration and tumor accumulation of DXR are shown in (A) and (B), respectively. Data are represented by mean ± S.D. ($n = 3$).

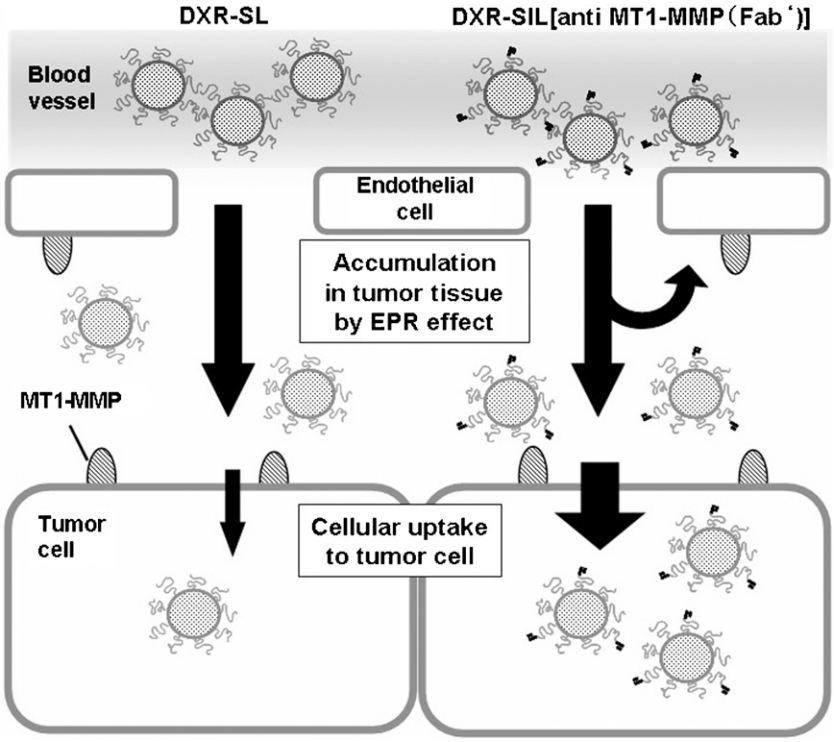

Fig. 5. Schematic diagram illustrating a possible mechanism for the tumor cell and/or neovascular cells by means of DXR-SIL[anti-MT1-MMP(Fab′)]. Since tumor accumulation of DXR-SIL[anti-MT1-MMP(Fab′)] was comparable to DXR-SL, DXR-SIL[anti-MT1-MMP(Fab′)] may accumulate in tumor mainly via EPR effect as is the case of DXR-SL. After they accumulate in the tissue, DXR-SIL[anti-MT1-MMP(Fab′)] efficiently internalize by virtue of a function of $Fab'_{222\text{-}1D8}$ modified on the distal end of PEG.

inconsistent with the previous observation that liposomes modified with peptides having binding activity to MT1-MMP showed highly tumor accumulation compared with non-targeting liposomal formulation (Kondo et al., 2004). It can be accounted for by assuming the difference of the investigation time after administration. In the previous peptide-modified liposomes, accumulation was evaluated just after injection. Then, contribution of EPR effect on tumor accumulation would be minor. However, in the present study, the tumor distribution was measured at 48 h after i.v. administration. Therefore, the liposomal accumulation in tumor may be mainly achieved by EPR effect, rather than active targeting via the specific antibody. Furthermore, considering the physiological role of MT1-MMP to digest the matrix, there is also the possibility that MT1-MMP was mainly expressed on the abluminal side but not on the apical side, and then both of DXR-SIL[anti-MT1-MMP(Fab′)] and DXR-SL accumulated to the tumor mainly via EPR effect. Once accumulated in the tumor tissue, $Fab'_{222\text{-}1DB}$ function as an accelerator for the cellular uptake of SIL[anti-MT1-MMP(Fab′)] by the neovascularity and tumor cells. In this sense, the Fab′ fragment contributed to controlling intra-tumor disposition of liposomes, but not to the tissue targeting in systemic circulation (Fig. 5).

4. Conclusion

Fab′ fragment ($Fab'_{222\text{-}1D8}$) against MT1-MMP was potent ligand, which may accelerate the cellular accumulation of doxorubicin-encapsulating sterically stabilized liposomes to the cancer cells and/or neovascular cells after they reached to the tumor tissue via EPR effect.

Acknowledgements

This work was supported in part by Grants-in-Aid for Scientific Research (B) and Grant-in-Aid for Young Scientists (B) from the Ministry of Education, Culture, Sports, Science and Technology of Japan, and by Grants-in-Aid for Scientific Research on Priority Areas from the Japan Society for the Promotion of Science.

References

Aoki, T., Yonezawa, K., Ohuchi, E., Fujimoto, N., Iwata, K., Shimada, T., Okada, Y., Seiki, M., 2002. Two-step sandwich enzyme immunoassay using monoclonal antibodies for detection of soluble and membrane-associated human membrane type 1-matrix metalloproteinase. J. Immunoassay Immunochem. 23, 49–68.

Čeh, B., Winterhalter, M., Frederik, P.M., Vallner, J.J., Lasic, D.D., 1997. Stealth liposomes: from theory to product. Adv. Drug Del. Rev. 24, 165–177.

Haran, G., Cohen, R., Bar, L.K., Barenholz, Y., 1993. Transmembrane ammonium sulfate gradients in liposomes produce efficient and stable entrapment of amphipathic weak bases. Biochim. Biophys. Acta 1151, 201–215.

Hatakeyama, H., Akita, H., Maruyama, K., Suhara, T., Harashima, H., 2004. Factors governing the *in vivo* tissue uptake of transferrin-coupled polyethylene glycol liposomes *in vivo*. Int. J. Pharm. 281, 25–33.

Huwyler, J., Wu, D., Pardridge, W.M., 1996. Brain drug delivery of small molecules using immunoliposomes. Proc. Natl. Acad. Sci. U.S.A. 93, 14164–14169.

Itoh, Y., Seiki, M., 2004. MT1-MMP: an enzyme with multidimensional regulation. Trends Biochem. Sci. 29, 285–289.

Klibanov, A.L., Maruyama, K., Torchilin, V.P., Hunag, L., 1990. Amphipathic polyethylenglycols effectively prolong the circulation time of liposomes. FEBS Lett. 268, 235–237.

Knauper, V., Will, H., Lopez-Otin, C., Smith, B., Atkinson, S.J., Stanton, H., Hembry, R.M., Murphy, G., 1996. Cellular mechanisms for human procollagenase-3 (MMP-13) activation. Evidence that MT1-MMP (MMP-14) and gelatinase a (MMP-2) are able to generate active enzyme. J. Biol. Chem. 271, 17124–17131.

Kondo, M., Asai, T., Sadzuka, Y., Katanasaka, Y., Ogino, K., Taki, T., Baba, K., Oku, N., 2004. Anti-neovascular therapy by liposomal drug targeted to membrane type-1 matrixmetalloproteinase. Int. J. Cancer 108, 301–306.

Lukyanov, A.N., Elbayoumi, T.A., Chakilam, A.R., Torchilin, V.P., 2004. Tumor-targeted liposomes: doxorubicin-loaded long-circulating liposomes modified with anti-cancer antibody. J. Control. Release 100, 135–144.

Maeda, N., Takeuchi, Y., Takada, M., Sadzuka, Y., Namba, Y., Oku, N., 2004. Anti-neovascular therapy by use of tumor neovasculature-targeted long-circulating liposomes. J. Control. Release 100, 41–52.

Maekawa, R., Maki, H., Yoshida, H., Hojo, K., Tanaka, H., Wada, T., Uchida, N., Takeda, Y., Kasai, H., Okamoto, H., Tsuzuki, H., Kambayashi, Y., Watanabe, F., Kawada, K., Toda, K., Ohtani, M., Sugita, K., Yoshioka, T., 1999. Correlation of antiangiogenic and antitumor efficacy of *N*-biphenyl sulfonyl-phenylalanine hydroxiamic acid (BPHA), an orally active, selective matrix metalloproteinase inhibitor. Cancer Res. 59, 1231–1235.

Maruyama, K., Takahashi, N., Tagawa, T., Nagaike, K., Iwatsuru, M., 1997. Immunoliposomes bearing polyethyleneglycol-coupled Fab′ fragment show prolonged circulation time and high extravasation into targeted solid tumors *in vivo*. FEBS Lett. 413, 177–180.

Matsumura, Y., Maeda, H., 1986. A new concept for macromolecular therapeutics in cancer chemotherapy: mechanism of tumoritropic accumulation of proteins and the antitumor agent smancs. Cancer Res. 46, 6387–6392.

Mendelsohnand, J., Baselga, J., 2003. Status of epidermal growth factor receptor antagonists in the biology and treatment of cancer. J. Clin. Oncol. 21, 2787–2799.

Nelson, N.J., 1998. Inhibitors of angiogenesis enter phase III testing. J. Natl. Cancer Inst. 90, 960–963.

Noel, A., Santavicca, M., Stoll, I., L'Hoir, C., Staub, A., Murphy, G., Rio, M.C., Basset, P., 1995. Identification of structural determinants controlling human and mouse stromelysin-3 proteolytic activities. J. Biol. Chem. 270, 22866–22872.

Ohuchi, E., Imai, K., Fujii, Y., Sato, H., Seiki, M., Okada, Y., 1997. Membrane type 1 matrix metalloproteinase digests interstitial collagens and other extracellular matrix macromolecules. J. Biol. Chem. 272, 2446–2451.

Pagenstecher, A., Stalder, A.K., Kincaid, C.L., Shapiro, S.D., Campbell, I.L., 1998. Differential expression of matrix metalloproteinase and tissue inhibitor of matrix metalloproteinase genes in the mouse central nervous system in normal and inflammatory states. Am. J. Pathol. 152, 729–741.

Pardridge, W.M., 2004. Intravenous, non-viral RNAi gene therapy of brain cancer. Expert Opin. Biol. Ther. 4, 1103–1113.

Pei, D., Weiss, S.J., 1996. Transmembrane-deletion mutants of the membrane-type matrix metalloproteinase-1 process progelatinase A and express intrinsic matrix-degrading activity. J. Biol. Chem. 271, 9135–9140.

Pei, D., Majmudar, G., Weiss, S.J., 1994. Hydrolytic inactivation of a breast carcinoma cell-derived serpin by human stromelysin-3. J. Biol. Chem. 269, 25849–25855.

Ponkaand, P., Lok, C.N., 1999. The transferrin receptor: role in health and disease. Int. J. Biochem. Cell Biol. 31, 1111–1137.

Qian, A.M., Li, H., Sun, H., ho, K., 2002. Targeted drug delivery via the transferrin receptor-mediated endocytosis pathway. Pharmacol. Rev. 54, 561–587.

Sato, H., Takino, T., Okada, Y., Cao, J., Shinagawa, A., Yamamoto, E., Seiki, M., 1994. A matrix metalloproteinase expressed on the surface of invasive tumour cells. Nature 370, 61–65.

Strongin, A.Y., Collier, I., Bannikov, G., Marmer, B.L., Grant, G.A., Goldberg, G.I., 1995. Mechanism of cell surface activation of 72-kDa type IV collagenase. Isolation of the activated form of the membrane metalloprotease. J. Biol. Chem. 270, 5331–5338.

Uekita, T., Itoh, Y., Yana, I., Ohno, H., Seiki, M., 2001. Cytoplasmic tail-dependent internalization of membrane-type 1 matrix metalloproteinase is important for its invasion-promoting activity. J. Cell Biol. 155, 1345–1356.

Voinea, M., Manduteanu, I., Dragomir, E., Capraru, M., Simionescu, M., 2005. Immunoliposomes directed toward VCAM-1 interact specifically with activated endothelial cells—a potential tool for specific drug delivery. Pharm. Res. 22, 1906–1917.

Wang, X., Ma, D., Keski-Oja, J., Pei, D., 2004. Co-recycling of MT1-MMP and MT3-MMP through the trans-Golgi network. Identification of DKV582 as a recycling signal. J. Biol. Chem. 279, 9331–9336.

Xu, L., Huang, C.C., Huang, W., Tang, W.H., Rait, A., Yin, Y.Z., Cruz, I., Xiang, L.M., Pirollo, K.F., Chang, E.H., 2002. Systemic tumor-targeted gene delivery by anti-transferrin receptor scFv-immunoliposomes. Mol. Cancer Ther. 1, 337–346.

Zhang, Y., Boado, R.J., Pardridge, W.M., 2003. Marked enhancement in gene expression by targeting the human insulin receptor. J. Gene Med. 5, 157–163.